ARTICLE

BIOTECHNOLOGY and BIOENGINEERING

A Microfluidic Bioreactor With Integrated Transepithelial Electrical Resistance (TEER) Measurement Electrodes for Evaluation of Renal Epithelial Cells

Nicholas Ferrell,[1] Ravi R. Desai,[2] Aaron J. Fleischman,[1] Shuvo Roy,[3] H. David Humes,[4] William H. Fissell[1,5]

[1]Cleveland Clinic, Department of Biomedical Engineering, 9500 Euclid Ave. ND 20, Cleveland, Ohio 44195; telephone: 216-445-2206; fax: 216-444-9198; e-mail: fisselw@ccf.org

[2]Cleveland Clinic, Lerner College of Medicine, Cleveland, Ohio

[3]Department of Bioengineering and Therapeutic Sciences, University of California, San Francisco, San Francisco, California

[4]Department of Internal Medicine, University of Michigan, Innovative Biotherapies Inc., Ann Arbor, Michigan

[5]Cleveland Clinic, Department of Nephrology and Hypertension, Cleveland, Ohio

Received 14 January 2010; revision received 24 May 2010; accepted 2 June 2010

Published online 15 June 2010 in Wiley Online Library (wileyonlinelibrary.com). DOI 10.1002/bit.22835

ABSTRACT: We have developed a bilayer microfluidic system with integrated transepithelial electrical resistance (TEER) measurement electrodes to evaluate kidney epithelial cells under physiologically relevant fluid flow conditions. The bioreactor consists of apical and basolateral fluidic chambers connected via a transparent microporous membrane. The top chamber contains microfluidic channels to perfuse the apical surface of the cells. The bottom chamber acts as a reservoir for transport across the cell layer and provides support for the membrane. TEER electrodes were integrated into the device to monitor cell growth and evaluate cell–cell tight junction integrity. Immunofluorescence staining was performed within the microchannels for ZO-1 tight junction protein and acetylated α-tubulin (primary cilia) using human renal epithelial cells (HREC) and MDCK cells. HREC were stained for cytoskeletal F-actin and exhibited disassembly of cytosolic F-actin stress fibers when exposed to shear stress. TEER was monitored over time under normal culture conditions and after disruption of the tight junctions using low Ca^{2+} medium. The transport rate of a fluorescently labeled tracer molecule (FITC-inulin) was measured before and after Ca^{2+} switch and a decrease in TEER corresponded with a large increase in paracellular inulin transport. This bioreactor design provides an instrumented platform with physiologically meaningful flow conditions to study various epithelial cell transport processes.

Correspondence to: William H. Fissell
Contract grant sponsor: Wildwood Foundation
Contract grant sponsor: National Institutes of Health
Contract grant number: 1 R01 EB008049-01
Contract grant sponsor: US Department of Defense
Contract grant number: W81XWH-05-2-0010
Additional Supporting Information may be found in the online version of this article.

Biotechnol. Bioeng. 2010;107: 707–716.

KEYWORDS: bioreactor; microfluidics; kidney; epithelial cells; transepithelial electrical resistance

Introduction

The tubular epithelium of the kidney is responsible for reabsorption of water, salts, and various organic compounds. These transport processes along the length of the kidney tubule are responsible for maintaining volume balance and fluid composition in the body. There are two transport pathways across the tubular epithelium: transcellular and paracellular. Transcellular transport occurs through active processes such as ion transport by membrane ion pumps and receptor-mediated endocytosis and exocytosis. Transport across the paracellular pathway is primarily regulated by the permeability of tight junctions (TJ) at cell-to-cell contacts (Massry and Glassock, 2001).

A well-established method of monitoring TJ integrity, monolayer formation, and paracellular permeability in polarized, transporting epithelial cells is measurement of transepithelial electrical resistance (TEER) (Cereijido et al., 1978; Martinez-Palomo et al., 1980). TEER measurement systems are available commercially (World Precision Instruments (WPI), Sarasota, FL) and have been integrated

into microfabricated cell culture platforms (Hediger et al., 2000, 2001). TEER has been used to study regulation of TJ formation and disassembly under various experimental conditions (Cereijido et al., 1978; D'Angelo Siliciano and Goodenough, 1988; Martinez-Palomo et al., 1980; Zheng and Cantley, 2007). TEER has also been used to evaluate various cell types as in vitro drug transport models (Artursson, 1990; Cho et al., 1989).

Many transport processes in the kidney are known to be regulated by fluid flow and shear stress (Duan et al., 2008; Du et al., 2004; Malnic et al., 1989; Satlin et al., 2001). Salt and water reabsorption in the proximal tubule are proportional to tubular flow rate. This flow-dependent reabsorption is essential in maintaining glomerulotubular balance. Various experimental evidence suggests that mechanical signals in the form of shear stress at the apical cell surface are transduced into biochemical signals that regulate solute and water transport as well as other cell behaviors (Du et al., 2005; Praetorius and Spring, 2001; Preisig, 1992). While the mechanism by which cells sense flow is still an active area of research, there is evidence to suggest that the primary cilia and/or microvilli may act as the cells' flow sensor (Du et al., 2004, 2005; Guo et al., 2000; Praetorius and Spring, 2002; Schwartz et al., 1997). Further evidence suggests that the cell cytoskeleton is actively involved in signal transduction, as marked changes in the distribution of F-actin and other cytoskeletal proteins are seen in cultured kidney cells after exposure to shear stress (Alenghat et al., 2004; Duan et al., 2008; Essig et al., 2001).

It would be advantageous to be able to investigate renal epithelial transport processes in an experimental system that more closely mimics the in vivo micro-architecture of the kidney, allows application of physiologically relevant fluid flow, provides a pathway for apical to basolateral transport of solutes and water, and permits measurement of TEER in real-time. One promising option for the development of such a system is the use of a microfluidic perfusion bioreactor. Microfluidic perfusion cultures have been used to study a variety of adherent cell lines for high-throughput cell assays (Hung et al., 2005; Lee et al., 2006), drug and toxin screening (Park and Shuler, 2003; Wang et al., 2007), and tissue engineering (Bettinger et al., 2006; Borenstein et al., 2002; Powers et al., 2002a,b). These systems offer a high degree of control over the cells' mechanical and chemical microenvironment and reduce reagent consumption. Several systems have been developed that allow long-term culture (>7 days) of mammalian cells (Chung et al., 2005; Kim et al., 2007; Leclerc et al., 2003; Tourovskaia et al., 2005). Various aspects of shear-dependent cell behavior and transport in renal epithelial cells have been studied using microfluidic devices (Jang and Suh, 2009; Wang et al., 2009).

We have developed and evaluated a microfluidic perfusion bioreactor to study kidney epithelial cells. A TEER measurement system has been integrated into a microfluidic device to provide real-time monitoring of polarized monolayer formation and simultaneous evaluation of cellular permeability. Human renal epithelial cells (HREC) and Madin–Darby canine kidney (MDCK) epithelial cells were grown in the device, and then stained via indirect immunofluorescence for markers of differentiated function (cilia and tight junction formation). HREC were stained for F-actin to evaluate shear-dependent changes in cytoskeletal phenotype. The Ca^{2+} switch technique (Cereijido et al., 1978) was used to disrupt TJ and effects on TEER and corresponding transport of inulin were measured. This device provides a novel platform to study polarized epithelial cells under conditions that more closely mimic the in vivo environment.

Materials and Methods

Bioreactor Design

Exploded and cross-sectional schematics of the bioreactor system are shown in Figure 1a and b. The bioreactor was designed to provide perfusion of culture medium over the apical surface of the cells with an underlying fluidic chamber to allow transport of fluid and solutes across the cell layer. A membrane, sandwiched between the two fluidic layers, acts as a substrate for cell growth and gives a pathway for transport between the layers. The top chamber of the bioreactor consists of eight parallel channels, each 4.30 cm long, 0.31 cm wide, and ~50 μm tall. In order to provide a uniform flow rate in each channel, the flow from a single inlet channel was sequentially split into the eight channels of the bioreactor using *t*-channels. An array of posts in the bottom chamber supports the membrane while providing a pathway for solute and fluid transport. Each post is 200 μm in diameter with 200 μm spacing between posts.

The bioreactor was designed to provide shear stress at the cell surface that approximates in vivo conditions. Published data on proximal tubule ultrastructure and flow rates in rats suggest a shear stress in the range of approximately 0.5–5 dyn/cm^2 under normal conditions (Chou and Marsh, 1987; Maunsbach et al., 1987). In the rectangular-shaped channels of the bioreactor, assuming fully developed, incompressible, laminar flow, the shear stress is a function of the channel geometry, flow rate, and fluid viscosity according to Equation (1) (Fox and McDonald, 1992).

$$\tau_w = \frac{6Q\mu}{h^2 w} \tag{1}$$

where τ_w is the shear stress at the top and bottom surfaces of the channel, μ is the fluid viscosity, Q is the volume flow rate, and h and w are the height and width of the channel, respectively. Viscosity was assumed to be 9.6×10^{-4} Pa s. For simple rectangular microchannels, this numerical approximation agrees quite well with three-dimensional computation fluid dynamics simulations (Lu et al., 2004). Effects due to the sidewalls of the channel cause variation in the shear stress near the channel edges. These effects have been estimated to be relevant approximately one sidewall height

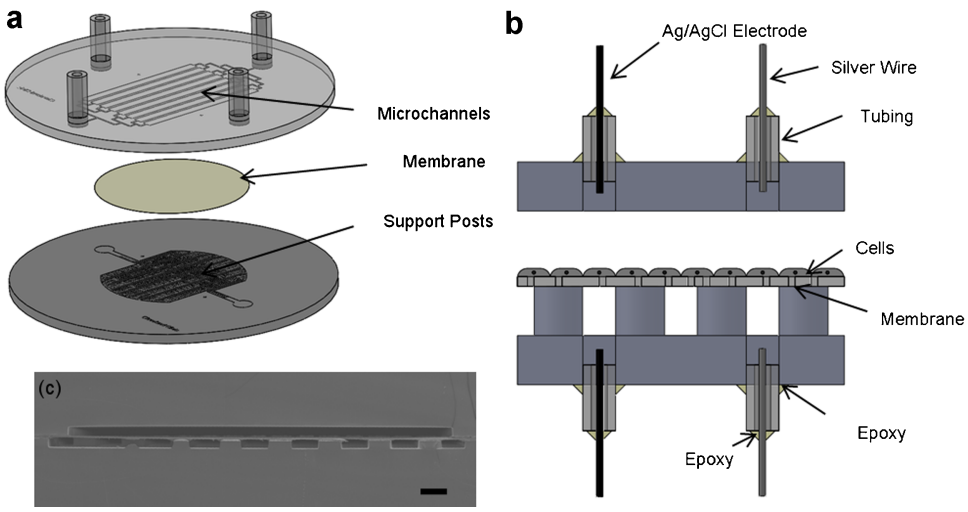

Figure 1. **a**: Exploded view of the bioreactor (TEER electrodes not shown), (**b**) schematic of the TEER electrode configuration consisting of a Ag/AgCl electrode and a Ag electrode on each side of the membrane, (**c**) cross-sectional scanning electron micrograph of the bioreactor. Scale bar in (c) is 200 μm. [Color figure can be seen in the online version of this article, available at wileyonlinelibrary.com.]

into the bulk fluid flow (Deen, 1998). Therefore, it is advantageous to have a channel with a small aspect ratio (AR), where AR is defined as the height of the channel divided by the width. As the AR decreases, uniform shear is maintained over a larger percentage of the top and bottom surfaces of the channel. Based on the channel dimensions used here, the shear stress is uniform over more than 95% of the channel surface.

Bioreactor Fabrication

Photoresist masters of the fluidic channels and support/collection chambers were fabricated using photolithography with either SU-8 2025 (Y111069, Microchem Corp., Newton, MA) or KMPR 1050 (Y211067, Microchem Corp.) photoresist. The photoresists were spin coated at 1,200 rpm (SU-8 2025) and 2,900 rpm (KMPR 1050). Wafers were then baked, exposed, and post-baked according to the manufacturer's suggested procedures. Photoresists were developed in SU-8 developer (Y020100, Microchem Corp.). After developing, the wafers were rinsed with isopropanol and dried with nitrogen.

Photoresist master patterns were transferred into polydimethylsiloxane (PDMS) which served as the structural material for the bioreactor. PDMS pre-polymer and curing agent (Sylgard 184, Dow Corning, Midland, MI) were mixed at a 10:1 ratio (w/w) and poured over the photoresist master. The PDMS was de-gassed in a vacuum desiccator and cured at 75°C for at least 6 h. After curing, the PDMS layers were removed from the photoresist masters and inlet/outlet holes were punched in the PDMS using a sheet metal press (No. 5 Jr. Hand Punch, Roper Whitney Co., Rockford, IL).

The membrane was fixed between the two fluidic layers using Loctite® medical grade epoxy (M121 HP, Henkel, Düsseldorf, Germany). The membrane was fixed to the bottom chamber of the device by contact printing a thin layer (~5 μm) of medical grade epoxy to the raised surface of the bottom chamber. The epoxy layer was printed by first applying the epoxy to a flat circular polystyrene blank ~50 mm in diameter. A glass roller was used to remove excess epoxy and flatten the epoxy into a smooth, thin layer. The epoxy-covered blank was then applied to the PDMS surface to transfer the epoxy onto the PDMS. Next, a Cyclopore™ polycarbonate membrane (7091-4710, Whatman, Inc., Florham Park, NJ) was attached to the epoxy-coated PDMS. This epoxy coating process was repeated on the top chamber of the device. Immediately after printing the epoxy to bond the membrane, the remaining uncoated PDMS surfaces were bonded by exposure to oxygen plasma (M4L, MetraLine/IPC, Corona, CA) for 1 min with an oxygen flow rate of 200 sccm, chamber pressure of 600 mTorr, and power of 200 W.

A variety of membranes could potentially be used for the bioreactor. We chose Cyclopore™ polycarbonate membranes for this study because they are thin, transparent, and are available with larger surface areas. The transparency of the membrane allows real-time optical imaging during bioreactor operation as well as in situ immunofluorescence imaging. Polycarbonate membranes are used in static membrane cell culture systems such as the Corning Transwell® system. Moreover, Cyclopore™ membranes have been shown to provide an adequate surface for epithelial cell culture (de Boer et al., 1994).

Tygon tubing (2.87 mm OD) (95609-30, Cole-Parmer, Vernon Hills, IL) was placed in the pre-punched holes and anchored with epoxy. The inlet/outlet holes were punched slightly smaller (~2.5 mm) than the OD of the tubing to create a press fit between the tubing and the PDMS to prevent epoxy from entering the inlet/outlet. Barbed female

polycarbonate luer fittings (1/16 in.) (45510-00, Cole-Parmer) were attached to the open end of the inlet/outlet tubes. The devices were sterilized by autoclave or ethylene oxide prior to cell seeding. Ethylene oxide sterilization was preferred because heating in the autoclave resulted in slight membrane deformation.

Bioreactor Characterization

Bioreactors were characterized by cross-sectional scanning electron microscopy (SEM). After assembly, the bioreactors were cross-sectioned with a razor blade. The sections were coated with a thin layer of gold in a sputter coater (SPI-Module, SPI Supplies, West Chester, PA). Devices were imaged on a JEOL (JSM-5310, Tokyo, Japan) scanning electron microscope. SEM was also used to measure the thickness of the epoxy layer. Measurements were taken on five devices.

The thickness of the microfluidic channels was measured using a mechanical stylus profilometer (3030, Dektak, Plainview, NY). For each device wafer, the average channel height was calculated from six measurements over the surface of the wafer. These measurements were used to adjust shear stress value based on inter-sample channel height variation and to evaluate the intra-sample shear distribution based on channel height variation over a single wafer. Using the average height for each device wafer, the flow rate necessary to achieve the desired shear stress in a single channel was calculated using Equation (1) then multiplied by the number of channels, and the pump flow rate was adjusted accordingly. The maximum thickness range for a single device wafer was used to calculate the largest expected variability in the shear stress due to variation in the channel geometry across the device.

To evaluate the adhesives used in the bioreactor assembly, burst pressure tests were performed in a manner similar to that described by Eddings et al. (2008). Detailed methods for conducting burst pressure tests can be found in the Supplementary Information.

Cell Culture

HREC were the kind gift of Innovative Biotherapies, Inc. (Ann Arbor, MI). The procedure for cell isolation was described previously (Humes et al., 1999a,b). Cells were at first or second passage at the time of freezing. Cells were maintained in freeze medium consisting of UltraMDCK medium (12-749Q, Lonza, Basel, Switzerland) with 10% (v/v) dimethylsulfoxide (DMSO) (D-2650, Sigma, St. Louis, MO) and stored in liquid nitrogen prior to use. Cells were quickly thawed and suspended in UltraMDCK medium supplemented with 1 mL/L insulin, transferrin, ethanolamine, and selenium (ITES) (17-839Z, Lonza), 0.7 μg/L triiodothyronine (T3) (T-6397, Sigma), 50 μg/L epidermal growth factor (EGF) (AF-100-15, Peprotech, Rocky Hill, NJ), 30 μg/L retinoic acid (RA) (R-2625, Sigma), and 10 mL/L antibiotic–antimycotic solution (15250, Invitrogen, Carlsbad, CA). This medium was used for all subsequent HREC cultures unless otherwise noted and is referred to as UltraMDCK with supplements. Cells were centrifuged at 300*g* for 5 min at 4°C followed by aspiration of the DMSO-containing medium. Cells were resuspended in fresh UltraMDCK medium with supplements and plated on culture surfaces at $2–5 \times 10^6$ cells per 100 mm diameter culture dish. Cells were incubated at 37°C with 5% CO_2. Culture medium was changed every other day as needed.

HREC culture surfaces were coated with murine collagen IV (354233, BD Biosciences, Bedford, MA) at 5 μg/cm^2. Stock collagen solutions were diluted in UltraMDCK without supplements and coating was performed for 1 h at room temperature. Culture surfaces were then coated with fetal bovine serum (FBS) (SH3007003, Thermo Fisher Scientific, Waltham, MA) for 4 h.

At confluence, cells were washed with phosphate-buffered saline (PBS) and detached from the culture plates using trypsin–versene (17-161E, Lonza) for ~10 min and no more than 20 min. An equal volume of trypsin inhibitor solution (1 g/L in PBS) (17075029, Invitrogen) was added to the trypsin–versene. Sterile cell scrapers were used to detach cells if needed. Cells were counted using a hemocytometer, centrifuged at 200*g* for 5 min at 4°C, resuspended in fresh UltraMDCK with supplements, and replated at $1–5 \times 10^6$ cells/plate.

MDCK cells were obtained from the American Type Culture Collection (ATCC) (CCL-34, Manassas, VA). Subculturing of MDCK cells was performed in a similar manner, but no supplements were added to the UltraMDCK medium with the exception of the antibiotic–antimycotic solution.

Perfusion Culture

Both the apical and basolateral chambers of the bioreactors were primed with the appropriate culture medium prior to seeding. In the case of the MDCK cells, no additional modification of the membrane was performed prior to cell seeding. For HREC cultures, membranes were coated with collagen IV prior to seeding. Both HREC and MDCK cells were seeded via a sterile syringe. HREC and MDCK cells were seeded at 2×10^7 cell/mL ($\sim 1 \times 10^5$ cells/cm^2) and 1×10^7 cells/mL ($\sim 5 \times 10^4$ cells/cm^2), respectively. The devices were placed in the incubator and cells were allowed to attach under static conditions for 4 h.

After cell attachment, the top chamber of the device was connected to the perfusion system. The perfusion system consisted of a media reservoir with stainless steel inlet/outlet tubes. Tygon tubing (2.87 mm OD) was connected to the media reservoir outlet and run through the perfusion pump (Masterflex C/L, Cole-Parmer). The tubing was then connected via barbed luer fittings to a 1 m length of 1.14 mm ID oxygen permeable platinum-cured silicone tubing (95612-30, Cole-Parmer). The silicone tubing was connected via luer fittings to the bioreactor. The outlet of the bioreactor

was connected to the medium reservoir via similar connections. The entire system was housed in an incubator at 37°C with 5% CO_2. The media reservoir was 75 mL and the media was changed every 5–6 days. Bioreactors were suspended above the incubator racks to facilitate gas diffusion from both sides of the device. The pump flow rate was set such that at cell confluence, a shear stress of ~1 dyn/cm^2 was achieved over the apical surface of the cells. This corresponded to pump flow rate of ~65 μL/min for a 50 μm tall array of eight channels. Adjustments were made to the flow rate based on the measured height of channels for each sample. The flow rate was held constant throughout the experiment after the initial 4 h attachment period. Cells were maintained in the perfusion bioreactor for at least 7 days prior to analysis. The inlet and outlet of the basolateral chamber were capped and clamped shut to prevent loss of medium during cell growth. The inlet and outlet were opened to allow sample collection and/or volume measurements.

Cell Characterization

During culture, the perfusion system and bioreactor were periodically removed from the incubator for phase contrast microscopy (AE 20, Motic, Xiamen, China). Images were taken with a digital camera (Powershot G9, Canon, Tokyo, Japan) attached to the microscope via an eyepiece adapter (Optem 257010, Qioptiq, Fairport, NY). Flow was generally stopped during inspection to allow easier handling. However, the bioreactor was not removed from the perfusion circuit at any time.

HREC and MDCK cells were stained for zona occludens-1 (ZO-1) membrane tight junction protein and acetylated α-tubulin (primary cilia). All immunofluorescence (IF) procedures were performed in situ within the microchannels by introducing the reagents into the channels via a syringe. Thorough washing with PBS was performed between each processing step. Cells were fixed with 4% paraformaldehyde (15700, Electron Microscopy Sciences, Harfield, PA) on ice for 20 min. Cells were then permeabilized with 0.1% Triton X-100 (LC26280-1, LabChem, Inc., Pittsburg, PA) for 10 min. A blocking buffer of 5% goat serum (16210-064, Invitrogen) in PBS with 0.1% sodium azide was introduced into the channels for 1 h. Rabbit anti-ZO-1 (40-2200, Invitrogen) and mouse anti-acetylated α-tubulin (32-2700, Invitrogen) antibodies were diluted 1:200 in blocking buffer and then introduced into the system and left static for 1 h. Cells were then incubated in the dark for 30 min in a secondary antibody mixture of Alexa Fluor 488 goat anti-rabbit IgG (A11008, Invitrogen) and Alexa Fluor 555 goat anti-mouse IgG (A21422, Invitrogen) at 1:200 in blocking buffer. Fluorescence images were obtained on an inverted fluorescence microscope (DM IRB, Leica, Wetzlar, Germany) with a digital camera (Regita-SRV, Q Imaging, Surrey, Canada). Fluorescence imaging was performed either through the PDMS layer, or a section of the PDMS was removed with a scalpel to provide access to the membrane. False colored images were overlaid using Image-Pro Discovery software (Media Cybernetics, Bethesda, MD).

Actin Staining

Cells were stained for F-actin after exposure to flow. Cells were initially perfused from the basolateral chamber for at least 5 days. Cells were then exposed to 1 dyn/cm^2 of fluid shear stress from the apical side for a period of 6 h. Static controls were grown to confluence on tissue culture polystyrene. Cells were washed with PBS and fixed with 4% paraformaldehyde for 20 min on ice. Cells were incubated in 1% bovine serum albumin (A7906, Sigma) for 30 min, then stained with 10 U/mL Alexa Fluor 555 phalloidin (A34055, Invitrogen) in the dark for 20 min. Nuclei were stained for 10 min using Vectashield® mounting media with 4′,6-diamidino-2-phenylindone (DAPI) (N1200, Vector Laboratories, Burlingame, CA).

Transepithelial Electrical Resistance (TEER)

The experimental setup for measuring TEER is shown in Figure 1b. Two 0.2 mm diameter Ag/AgCl wire electrodes (540800, A-M Systems, Sequim, WA) and two silver wire electrodes were inserted into 0.51 mm ID tygon tubing (95609-18, Cole-Parmer) so that the ends of the electrodes were exposed. The electrodes were fixed in place with epoxy. Prior to final bioreactor assembly, holes were punched in both PDMS layers and the electrode assemblies were inserted and anchored with epoxy. Bioreactors were then assembled and sealed as described in the bioreactor fabrication section. Electrodes were attached via an electrode adapter module (#3993, WPI) to an epithelial voltage/resistance meter (EVOMX, WPI).

The apical and basolateral chambers of the bioreactors were primed with cell culture medium and a blank membrane resistance was measured. Cells were seeded and perfused as described previously. Resistance measurements were taken daily. The resistance measurements were normalized to account for channel area (1.3 cm^3) resulting in units of Ω-cm^2. The blank resistance was then subtracted from the measured resistance to obtain the effective TEER.

Calcium Switch

To evaluate the TEER measurement system's ability to detect transient changes in resistance based on disruption of the permeability barrier (TJ), the calcium switch technique was used. Calcium is known to play a significant role in assembly and maintenance of tight junctions (Cereijido et al., 1978; Martinez-Palomo et al., 1980). MDCK cells were grown to confluence as described previously. Normal culture medium (UltraMDCK) was replaced with a low Ca^{2+} medium consisting of SMEM (11380, Invitrogen) with 3 mM ethylene diamine tetraacetic acid (EDTA) (118432500, Acros,

Geel, Belgium) to chelate any additional Ca^{2+}. TEER was measured every minute using the system described previously. Cells were then either prepared for ZO-1 and acetylated α-tubulin immunofluorescence or the medium was switched back to Ca^{2+}-containing medium and the cells were allowed to recover for 19 h and the resistance was measured after recovery.

The rate of inulin transport across the cell layer was measured before and after introducing low Ca^{2+} medium. FITC-labeled inulin (F3272, Sigma) was dissolved in UltraMDCK medium at 100 μg/mL. The medium was perfused at a pump inlet flow rate of 100 μL/min. The outlet flow was collected and the flow rate was calculated. The concentration of FITC-inulin in the outlet medium was then measured using a fluorescent plate reader with 485 nm excitation and 535 nm emission. The inulin leak rate was calculated by multiplying the inlet and outlet flow rates by their respective FITC-inulin concentrations to obtain the inlet and outlet inulin mass flow rates (μg/min). Subtracting the inlet and outlet mass flow rates yields the transmembrane mass flow rate (μg/min). This value was then divided by the total membrane area to give the inulin leak rate ($\mu g\,cm^{-2}\,min^{-1}$).

Results and Discussion

The bioreactor and its performance were characterized in three general steps. First, the bioreactor fabrication process and final device geometry and robustness were evaluated using traditional materials characterization techniques. Next, cells were introduced into the system and evaluated using standard optical microscopy and immunofluorescence staining for cell-specific phenotypic markers. Finally, the TEER measurement system was evaluated using normal cells and using a Ca^{2+} switch model, a standard model for TJ disruption.

The bioreactor geometry and robustness were evaluated using scanning electron microscopy, profilometry, and burst pressure measurements. It is important to properly evaluate the channel geometry, particularly for the apical flow channels, since small changes in height can lead to significant differences in the calculated shear stress. A cross-sectional scanning electron micrograph of the bioreactor is shown in Figure 1c. The bioreactor is ~100 mm in diameter and 3 mm thick (1.5 mm per side). The PDMS posts in the basolateral chamber of the device provided adequate support for the membrane. While a small amount of membrane deflection was observed, likely due to stresses during the fabrication and sterilization process, this did not appear to have any observable effect on cell attachment and spreading on the membrane surface. Thickness of the epoxy adhesive layer was 4.9 ± 1.4 μm (±standard deviation (SD), $n = 5$) as measured by SEM. Since non-traditional epoxy bonding was used to seal the membrane, it was necessary to evaluate the quality of the adhesive bond. Results of burst pressure tests can be found in the Supplementary Information. The epoxy exhibited adequate adhesion for this application. Based on the channel height measurements, the maximum range associated with the thickness measurements (7 μm) was

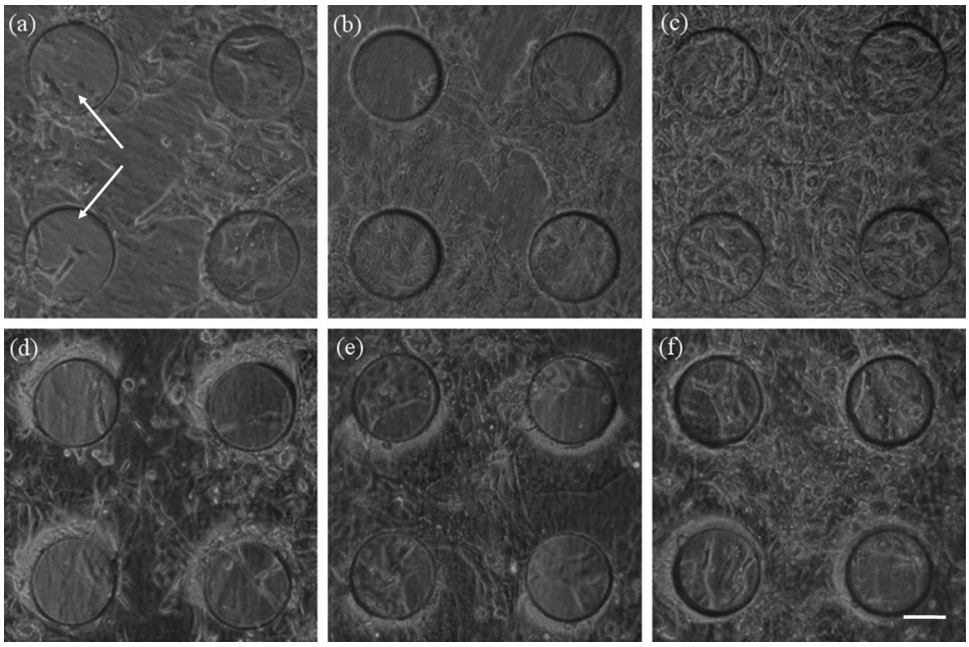

Figure 2. Optical micrographs of (**a–c**) MDCK cells at 1, 3, and 6 days of culture, respectively, and (**d–f**) HREC at 1, 6, and 10 days of culture, respectively. Support pillar underlying the membrane are indicated by arrows in (a). Note that the MDCK and HREC cells are at confluence in (c) and (f), respectively. Scale bar is 100 μm.

used to estimate maximum expected shear variation based on channel thickness variation. For a 50 μm tall channel this would result in a shear stress variation of approximately ±12%. It should be noted that the thickness range and corresponding shear stress variation for most devices was much less than the maximum.

Cell attachment and growth on the membrane were initially assessed qualitatively using standard phase contrast microscopy to ensure that the cells were able to attach to the membrane and grow to confluence under the bioreactor growth conditions. This highlights one of the main advantages of this system, as it can be difficult to view cells in traditional bioreactors since they are often non-transparent, non-planar, and too thick to view using standard, real-time microscopy techniques. Optical phase contrast micrographs of HREC and MDCK cells are shown at different culture times in Figure 2. Figure 2a–c shows MDCK cells at times of 1, 3, and 6 days, respectively. The images demonstrate that the cells were able to attach to the membrane and proliferated over time to form a monolayer. MDCK cells typically reached confluence 3–5 days after seeding. Figure 2d–f shows HREC at 1, 6, and 10 days, respectively. HREC took longer to reach confluence, even at higher seeding density. This is primarily a result of the difference in doubling time between an immortalized cell line (MDCK) and a primary cell line (HREC).

In addition to cell growth to confluence in the bioreactor, two important markers of differentiated cell function that are involved in tubular transport were accessed. ZO-1 was used to evaluate tight junction formation and acetylated α-tubulin was used as a marker of cilia formation. Tight junctions are critical for regulating paracellular transport while cilia have been implicated in flow-dependent cell signaling (Fissell et al., 2006; Nauli et al., 2001). Immunofluorescence micrographs of MDCK cells and HREC are shown in Figure 3a and b. Both cell types consistently stained positive for ZO-1 and acetylated α-tubulin, indicating tight junction and cilia formation. All steps in the

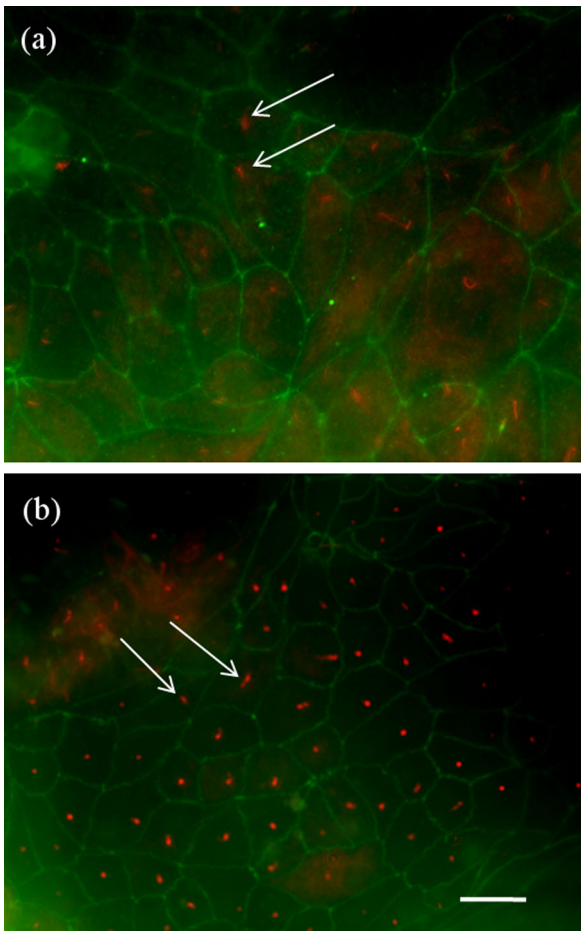

Figure 3. Fluorescence micrographs of (**a**) MDCK and (**b**) HREC following immunofluorescence staining for ZO-1 (tight junctions) and acetylated α-tubulin (primary cilia). Arrows indicate the primary cilia and tight junctions. Scale bar is 25 μm. [Color figure can be seen in the online version of this article, available at wileyonlinelibrary.com.]

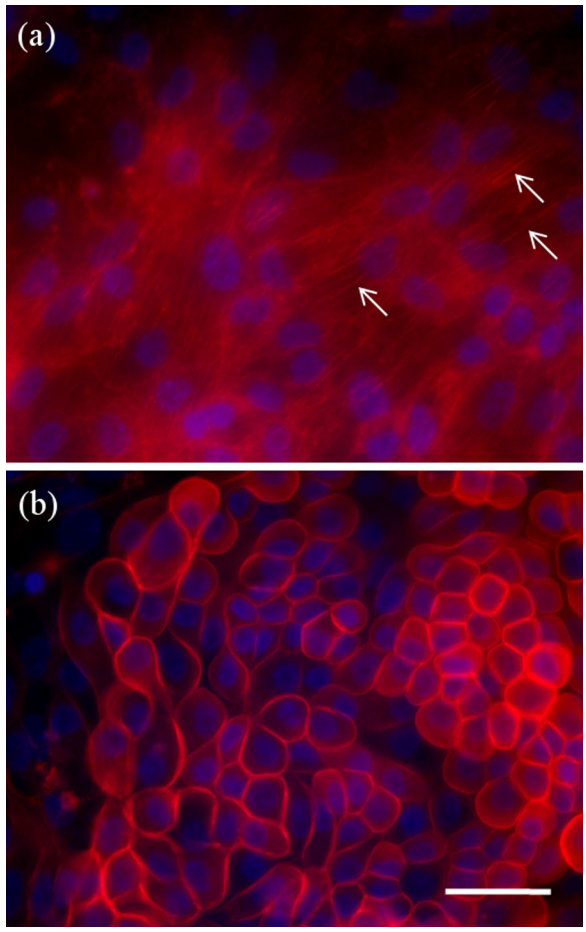

Figure 4. HREC stained for F-actin (**a**) under static conditions and (**b**) after 6 h of exposure to ~1 dyn/cm^2 fluid shear stress. Significant banding of F-actin is observed in the cytoplasm of the control cells. Stress fibers are indicated with arrows in (a). Under shear, F-actin reorganizes at the periphery of the cells. Scale bar is 25 μm. [Color figure can be seen in the online version of this article, available at wileyonlinelibrary.com.]

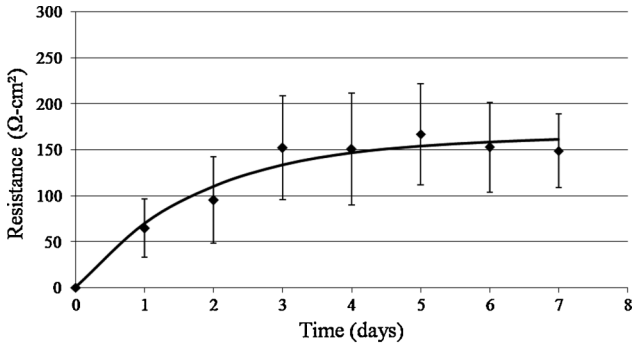

Figure 5. Transepithelial electrical resistance (TEER) versus time for MDCK cells grown in the bioreactor. A curve was fit to the data using an exponential rise to maximum function of the form $R = a(1 - e^{-bt})$, where R is resistance and t is time.

IF procedure were performed in situ within the microfluidic channels. Therefore, fluorescence imaging can be done without disassembling the device.

Fluorescence staining with Alexa Fluor 555 phalloidin revealed significant rearrangement of cytoskeletal F-actin in HREC after exposure to shear stress. Typical cytoskeletal actin fibers were seen in static cultures as seen in Figure 4a. After exposure to 1 dyn/cm^2 shear for 6 h, cells showed diminished cytocolic F-actin stress fibers and an increase in F-actin at the periphery of the cell (Fig. 4b). This is similar to results seen in MDCK and mouse proximal tubule epithelial cells after exposure to shear stress (Duan et al., 2008; Essig et al., 2001). Duan et al. (2008) suggest that this actin rearrangement is strong evidence for the role of the cytoskeleton in shear-induced mechanotransduction in renal epithelial cells. The data here suggests that this is also seen in cells of human origin.

Figure 5 shows a plot of the TEER versus time for MDCK cells grown in the bioreactor. The data are the mean resistance ± SD ($n = 5$). The data are fitted to an exponential curve of the form $R = a(1 - e^{-bt})$, where R is resistance and t is time. Stabilization of the resistance and corresponding cell confluence were in qualitative agreement with optical inspection. Differences in steady-state resistance may be a result of various experiment factors. However, the range of TEER measured in this study is similar to that measured by others for MDCK cells (Cho et al., 1989; Irvine et al., 1998). Following the experiment, the cells were removed from the membrane by trypsinization. The resistance was measured and the values were similar to the readings obtained from the blank membranes prior to cell seeding.

A classic model of tight junction disruption, the Ca^{2+} switch, was used to evaluate the TEER measurement system. Figure 6 shows the effect of low Ca^{2+} medium on TEER and inulin transport ($n = 3$, ±SD). Transepithelial resistance dropped significantly after introducing low Ca^{2+} medium as shown in Figure 6a. Resistance dropped to around 45% of the initial resistance after ~10 min. Cells that were allowed to recover by introducing normal Ca^{2+}-containing medium showed an increase in TEER to ~85% of the initial value after 19 h of recovery time. The rate of FITC-inulin transport (inulin leak rate) was measured before and after introducing low Ca^{2+} medium. Inulin was used as a marker for

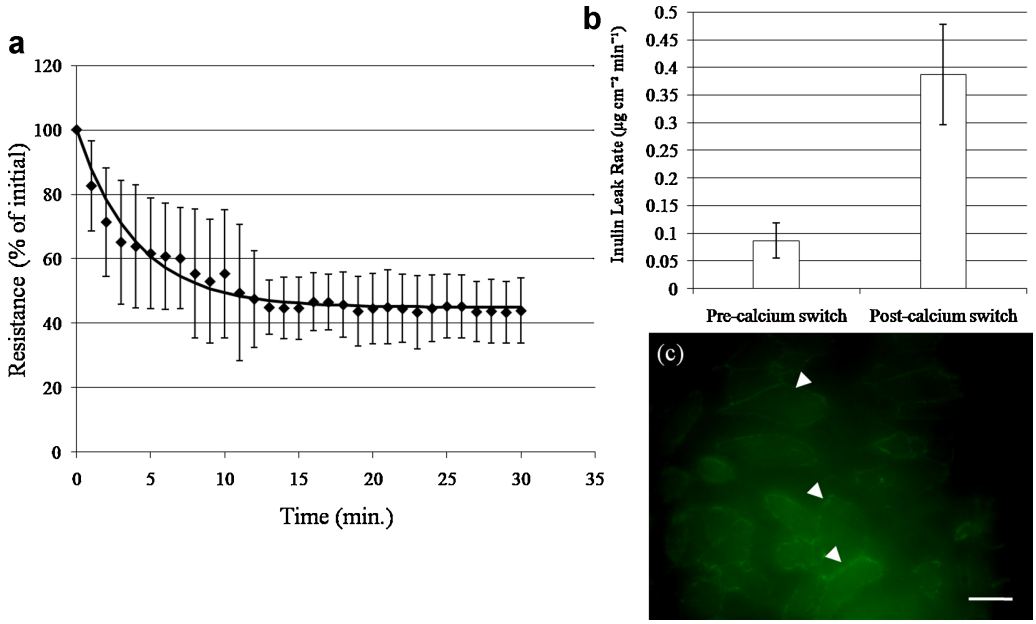

Figure 6. Results of Ca^{2+} switch on TEER and FITC-inulin transport. **a**: Decrease in TEER after Ca^{2+} switch. Low calcium medium was added at time 0. A curve was fit to the data with an exponential decay function of the form $R = R_o + a(e^{-bt})$, where R is resistance and t is time. **b**: Rate of inulin transport across the cell layer before and after Ca^{2+} switch. **c**: Immunofluorescence staining for ZO-1 after calcium switch showing breakdown in cell–cell contacts and diffuse, fragmented ZO-1 staining. Scale bar is 25 μm. [Color figure can be seen in the online version of this article, available at wileyonlinelibrary.com.]

paracellular transport due to its relatively low cellular uptake (Schwegler et al., 1991). Under normal conditions, the inulin leak rate was $0.09 \pm 0.03\,\mu g\,cm^{-2}\,min^{-1}$ and after adding low Ca^{2+} medium for 30 min the leak rate increased to $0.39 \pm 0.09\,\mu g\,cm^{-2}\,min^{-1}$ ($n = 3$, $\pm$SD), approximately a fourfold increase in permeability. Figure 6c shows IF staining post-Ca^{2+} switch. Some ZO-1 staining is still observed at the perimeter of the cells as indicated by the arrows, although much more fragmented. The image shows that the cell–cell contacts have begun to break down and some cells were removed from the surface.

Conclusions

We developed a bilayer microfluidic bioreactor with integrated TEER electrodes for studying kidney epithelial cells. HREC and MDCK cells were grown in the bioreactor under perfusion. Differentiated function (i.e., cilia and tight junction formation) was demonstrated with both cell types. Phenotypic changes (F-actin cytoskeletal reorganization) were observed in human cells in response to shear stress. The TEER measurement system was used to evaluate formation of a polarized monolayer of cells. The device was also used to measure changes in TEER and inulin transport after disruption of tight junctions by Ca^{2+} switch. This experimental system can be used to study a wide range of flow-dependant processes in renal epithelial cells.

This work was supported by the Wildwood Foundation, the National Institutes of Health (1 R01 EB008049-01), and the US Department of Defense (W81XWH-05-2-0010). NF is funded by a training grant from the National Institutes of Health (2 T32 DK007470-27). The authors would like to thank Anna Dubnisheva (Cleveland Clinic), Eun Jung Kim (Cleveland Clinic), Ross Smith (Cleveland Clinic), and Angela Westover (Innovative Biotherapies, Inc.) for technical assistance.

Disclosure

HDH is a shareholder in Innovative Biotherapies Inc., a spin-out company of the University of Michigan.

References

Alenghat FJ, Nauli SM, Kolb R, Zhou J, Ingber DE. 2004. Global cytoskeletal control of mechanotransduction in kidney epithelial cells. Exp Cell Res 301:23–30.

Artursson P. 1990. Epithelial transport of drugs in cell culture. I: A model for studying the passive diffusion of drugs over intestinal absorbtive (Caco-2) cells. J Pharm Sci 79:476–482.

Bettinger CJ, Weinberg EJ, Kulig KM, Vacanti JP, Wang Y, Borenstein JT, Langer R. 2006. Three-dimensional microfluidic tissue-engineering scaffolds using a flexible biodegradable polymer. Adv Mater 18:165–169.

Borenstein JT, Terai H, King KR, Weinberg EJ, Kaazempur-Mofrad MR, Vacanti JP. 2002. Microfabrication technology for vascularized tissue engineering. Biomed Microdevices 4:167–175.

Cereijido M, Robbins ES, Dolan WJ, Rotunno CA, Sabatini DD. 1978. Polarized monolayers formed by epithelial cells on a permeable and translucent support. J Cell Biol 77:853–880.

Cho MJ, Thompson DP, Cramer CT, Vidmar TJ, Scieszka JF. 1989. The Madin Darby canine kidney epithelial cell monolayer as a model cellular transport barrier. Pharm Res 6:71–77.

Chou CL, Marsh DJ. 1987. Measurement of flow rate in rat proximal tubules with a nonobstructing optical method. Am J Physiol Renal Physiol 253:F366–F371.

Chung BG, Flanagan LA, Rhee SW, Schwartz PH, Lee AP, Monuki ES, Jeon NL. 2005. Human neural stem cell growth and differentiation in a gradient-generating microfluidic device. Lab Chip 5:401–406.

D'Angelo Siliciano J, Goodenough DA. 1988. Localization of the tight junction protein, ZO-1, is modulated by extracellular calcium and cell-cell contact in Madin-Darby canine kidney epithelial cells. J Cell Biol 107:2389–2399.

de Boer WI, Rebel JMJ, Vermey M, Thijssen CDEM, van der Kwast TH. 1994. Muliparameter analysis of primary epithelial cultures grown on cyclopore membranes. J Histochem Cytochem 42:277–282.

Deen W. 1998. Analysis of transport phenomenon. New York: Oxford University Press.

Du Z, Daun Y, Yan Q, Weinstein AM, Weinbaum S, Wang T. 2004. Mechanosensory function of microvilli of the kidney tubule. Proc Natl Acad Sci USA 101:13068–13073.

Du Z, Yan Q, Daun Y, Weinbaum S, Weinstein AM, Wang T. 2005. Axial flow modulates proximal tubule NHE3 and H-ATPase activities by changing microvillus bending moments. Am J Physiol Renal Physiol 290:F289–F296.

Duan Y, Gotoh N, Yan Q, Du Z, Weinstein AM, Wang T. 2008. Shear-induced reorganization of renal proximal tubule cell actin cytoskeleton and apical junctional complexes. Proc Natl Acad Sci USA 105:11418–11423.

Eddings MA, Johnson MA, Gale BK. 2008. Determining the optimal PDMS-PDMS bonding technique for microfluidic devices. J Micromech Microeng 18:1–4.

Essig M, Terzi F, Burtin M, Friedlander GF. 2001. Mechanical strains induced by tubular flow affect the phenotype of proximal tubular cells. Am J Physiol Renal Physiol 281:F751–F762.

Fissell WH, Manley S, Westover A, Humes HD, Fleischman AJ, Roy S. 2006. Differentiated growth of human renal tubule cells on thin-film and nanostructured materials. ASAIO J 52:221–227.

Fox RW, McDonald AT. 1992. Introduction to fluid mechanics. New York: John Wiley and Sons.

Guo P, Weinstein AM, Weinbaum S. 2000. A hydrodynamic mechanosensory hypothesis for brush border microvilli. Am J Physiol Renal Physiol 279:F698–F712.

Hediger S, Fontannaz J, Sayah A, Hunziker W, Gijs MAM. 2000. Biosystem for the culture and characterisation of epithelial cell tissues. Sensor Actuat B Chem 63:63–73.

Hediger S, Sayah A, Horisberger JD, Gijs MAM. 2001. Modular microsystem for epithelial cell culture and electrical characterisation. Biosens Bioelectron 16:689–694.

Humes HD, McKay SM, Funke AJ, Buffington DA. 1999a. Tissue engineering of a bioartificial renal tubule assist device: In vitro transport and metabolic characteristics. Kidney Int 55:2502–2514.

Humes HD, Buffington DA, McKay SM, Funke AJ, Weitzel WF. 1999b. Replacement of renal function in uremic animals with a tissue-engineered kidney. Nat Biotechnol 17:451–455.

Hung PJ, Lee PJ, Sabounchi P, Lin R, Lee LP. 2005. Continuous perfusion microfluidic cell culture array for high-throughput cell-based assays. Biotechnol Bioeng 89:1–8.

Irvine JD, Takahashi L, Lockhart K, Cheong J, Tolan JW, Selick HE, Grove JR. 1998. MDCK (Madin-Darby canine kidney) cells: A tool for membrane permeability screening. J Pharm Sci 88:28–33.

Jang K-J, Suh K-Y. 2009. A multi-layer microfluidic device for efficient culture and analysis of renal tubular cells. Lab Chip 10:36–42.

Kim L, Toh Y-C, Voldman J, Yu H. 2007. A practical guide to microfluidic perfusion culture of adherent mammalian cells. Lab Chip 7:681–694.

Leclerc E, Sakai Y, Fujii T. 2003. Cell culture in 3-dimensional microfluidic structure of PDMS (polydimethylsiloxane). Biomed Microdevices 5: 109–114.

Lee PJ, Hung PJ, Rao VM, Lee LP. 2006. Nanoliter scale microbioreactor array for quantitative cell biology. Biotechnol Bioeng 94: 5–14.

Lu H, Koo LY, Wang WM, Lauffenburger DA, Griffith LG, Jensen KF. 2004. Microfluidic shear device for quantitative analysis of cell adhesion. Anal Chem 76:5257–5264.

Malnic G, Berliner RW, Giebisch G. 1989. Flow dependence of K+ secretion in cortical distal tubules of the rat. Am J Physiol Renal Physiol 256: F932–F941.

Martinez-Palomo A, Meza I, Beaty G, Cereijido M. 1980. Experimental modulation of occluding junctions in a cultured transporting epithelium. J Cell Biol 87:736–745.

Massry SG, Glassock RJ. 2001. Textbook of nephrology. Philadelphia: Lippincott Williams & Wilkins.

Maunsbach AB, Giebisch GH, Stanton BA. 1987. Effects of flow rate on proximal tubule ultrastructure. Am J Physiol Renal Physiol 253:F582–F587.

Nauli SM, Alenghat FJ, Lu Y, William E, Vassilev P, Li X, Elia AEH, Lu W, Brown EM, Quinn SJ, Ingber DE, Zhou J. 2001. Polycystins 1 and 2 mediate mechanosensation in the primary cilium of kidney cells. Nat Genet 33:129–137.

Park TH, Shuler ML. 2003. Integration of cell culture and microfabrication technology. Biotechnol Prog 19:243–253.

Powers MJ, Janigian DM, Wack KE, Baker CS, Beer Stolz D, Griffith LG. 2002a. Functional behavior of primary rat liver cells in a three-dimensional perfused microarray bioreactor. Tissue Eng 8:499–513.

Powers MJ, Domansky K, Kaazempur-Mofrad MR, Kalezi A, Capitano A, Upadhyaya A, Kurzawski P, Wack KE, Stolz DB, Kamm R, Griffith LG. 2002b. A microfabricated array bioreactor for perfused 3D liver culture. Biotechnol Bioeng 78:257–269.

Praetorius HA, Spring KR. 2001. Bending the MDCK cell primary cilium increases intracellular calcium. J Membr Biol 184:71–79.

Praetorius HA, Spring KR. 2002. Removal of the MDCK cell primary cilium abolishes flow sensing. J Membr Biol 191:69–76.

Preisig PA. 1992. Luminal flow rate regulates proximal tubule H-HCO_3 transporters. Am J Physiol Renal Physiol 262:F47–F54.

Satlin LM, Sheng S, Woda GB, Kleyman TR. 2001. Epithelial Na+ channels are regulated by flow. Am J Physiol Renal Physiol 280:F1010–F1018.

Schwartz EA, Leonard ML, Bizios R, Bowser SS. 1997. Analysis and modelling of the primary cilium bending response to fluid shear. Am J Physiol Renal Physiol 272:F132–F138.

Schwegler JS, Heppelmann B, Mildenberger S, Silbernag S. 1991. Receptor-mediated endocytosis of albumin in cultured opossum kidney cells: A model for proximal tubular protein reabsorption. Eur J Physiol 418: 383–392.

Tourovskaia A, Figueroa-Masot X, Folch A. 2005. Differentiation-on-a-chip: A microfluidic platform for long-term cell culture studies. Lab Chip 5:14–19.

Wang Z, Kim MC, Marquez M, Thorsen T. 2007. High-density microfluidic arrays for cell cytotoxicity analysis. Lab Chip 7:740–745.

Wang J, Jeo J, Hua SZ. 2009. Spatially resolved shear distribution in microfluidic chip for studying force transduction mechanisms in cells. Lab Chip 10:235–239.

Zheng B, Cantley LC. 2007. Regulation of epithelial tight junction assembly and disassembly by AMP-activated protein kinase. Proc Natl Acad Sci 104:819–822.